Carbohydrate Polymers 278 (2022) 118958

Contents lists available at ScienceDirect

Carbohydrate Polymers

journal homepage: www.elsevier.com/locate/carbpol

Optimized hydration dynamics in mucoadhesive xanthan-based trilayer vaginal films for the controlled release of tenofovir

Araceli Martín-Illana [a], Eva Chinarro [b], Raul Cazorla-Luna [a], Fernando Notario-Perez [a], M. D. Veiga-Ochoa [a], Juan Rubio [b], Aitana Tamayo [b,*]

[a] Department of Pharmaceutics and Food Technology, Faculty of Pharmacy, Universidad Complutense de Madrid, Plaza Ramón y Cajal s.n, 28007 Madrid, Spain
[b] Institute of Ceramics and Glass, CSIC, Kelsen 5, 28049 Madrid, Spain

ARTICLE INFO

Keywords:
HIV
Electrochemical impedance spectroscopy
Hydration dynamics
Swelling
Drug release

ABSTRACT

Karaya gum, pectin and xanthan gum have been tested as candidates for manufacturing mucoadhesive trilayer films containing ethylcellulose and chitosan for the vaginal administration of the antiviral Tenofovir (TFV). The swelling profile correlated with the amount of mobile dipoles determined by impedance spectroscopy allows the determination of the hydration dynamics of these films. The fast water penetration has been demonstrated to favor the formation of polyelectrolyte complexes (PEC) via hydrogen or ionic bonds which would favor a controlled release. The incorporation of an inorganic drug release regulator induces the weakness of the polymeric chains thus enhancing the ionic mobility via the formation of low molecular weight PECs in films manufactured with karaya gum. Due to the different mechanical properties of the individual components, pectin-based films failed for a potential pharmaceutical formulation. However, mucoadhesive trilayer films produced with xanthan gum have demonstrated a moderate swelling, improved wettability and a controlled release of TFV.

1. Introduction

Forty years after the first reported AIDS cases, HIV infection continues being a serious public health problem affecting millions of people worldwide. A recent UNAIDS report (UNAIDS_Secretary_General, 2021) highlights the problem of inequalities -especially gender- that increase the vulnerability of certain population groups towards infection. The limitations of women's power to make decisions related to their sexual health and their access to sexual health services allow explaining that reducing the risk of contracting HIV infection is not under their control. On the other hand, the report reveals the importance of prioritizing prevention to ensure that as many people at risk as possible have effective tools available in the coming years to reduce the high number of new cases of HIV infection at present.

Vaginal microbicides containing inhibitors for the replication of the reverse transcriptase of the HIV have made remarkable progress in biomedicine, showing efficacy in the prevention of HIV-1 infection (Karim et al., 2010). However, the lack of efficacy observed in several clinical trials justifies the need for the development of new formulations (Cost et al., 2012). Antiretroviral-loaded vaginal films emerge as an option with promising features for the prevention of the sexual transmission of HIV (Fan et al., 2017; Notario-Pérez et al., 2020). Vaginal films are polymeric thin sheets which contain the drug dissolved or dispersed that dissolve or disintegrate quickly in contact with body fluids. Some of the advantages of the films as drug-loaded vaginal formulations include their low weight, high adhesiveness, and their ability to form an encapsulating polymeric matrix which helps regulating the drug release (Mesquita et al., 2019; Notario-Pérez et al., 2020).

A highly attractive solution to improve the characteristics of the vaginal films as drug delivery platforms are multilayer films. The properties provided by each layer to the whole system increase their versatility, for instance allowing enhanced mucoadhesion and a modulated response in drug delivery. Although the obtaining of multilayer films for vaginal administration has not been deeply explored, it is possible to find some recent references. Cazorla-Luna, Martin-Illana, Notario-Perez, Bedoya, et al. (2020) prepared layer-by-layer films consisting on a highly mucoadhesive layer based on chitosan derivatives — to be in contact with the vaginal tissue — and an external layer based on the pH responsive polymer Eudragit® S100. These authors (Cazorla-Luna, Notario-Perez, Martin-Illana, Bedoya, et al., 2020) also proposed the manufacturing of bilayer films in a single-step process for the first time. These films were composed by ethylcellulose as controlled release

* Corresponding author at: Institute of Ceramics and Glass, Spanish National Research Council, Kelsen 5, 28049 Madrid, Spain.
E-mail address: aitanath@icv.csic.es (A. Tamayo).

https://doi.org/10.1016/j.carbpol.2021.118958
Received 26 August 2021; Received in revised form 29 October 2021; Accepted 28 November 2021
Available online 2 December 2021

polymer and a natural gum (xanthan gum or tragacanth gum) as mucoadhesive polymer.

Based on previous investigations (Notario-Pérez et al., 2020), the polymers selected in the present work were ethylcellulose, karaya gum, pectin, xanthan gum and chitosan. Cellulose derivatives are widely used in the design of drug delivery systems owing excellent film-forming abilities (Notario-Pérez et al., 2020). Films coatings based on ethylcellulose are commonly used as drug release regulators in many pharmaceutical dosage forms (Cazorla-Luna, Notario-Pérez, Martín-Illana, Bedoya, et al., 2020; Melegari et al., 2016). Pectin (from plants), xanthan gum (from bacteria) and chitosan (from animals) are polysaccharides widely used in the manufacture of vaginal films (Notario-Pérez et al., 2020). On its side, karaya gum is a branched polysaccharide obtained from plant sources that has not been widely studied as film-forming material so far (Cao & Song, 2019) and just a few works dealing with vaginal films have emerged recently (Martín-Illana et al., 2021).

The promising results obtained from these previous works arose in merging both techniques to obtain mucoadhesive and controlled drug release trilayer films. Just few examples of trilayer films for drug delivery can be found in the literature. As an example, Lei et al. (2011) formulated trilayered films based on poly(ε-caprolactone) as film-forming excipient and 5-fluorouracil as drug which was placed in the middle layer. The single layers were prepared using an extruder and the trilayer structure was obtained by subjecting the single layers under pressure using toluene as binder. On their side, Wang et al. (2020) prepared trilayer films with a dextran-based interlayer obtained by electrospinning and gelatin based outer layers manufactured by electrospinning or by solvent casting, applying hot-pressing for achieving the trilayer structure in the last case.

Inorganic and organic porous materials have been widely studied as excipients for the loading of drugs in order to obtain controlled drug delivery systems (Martin-Illana et al., 2020). The combination of organic and inorganic components allows to gain hybrid materials that meet not only the characteristics of both types of materials, but also a synergistic effect that makes them promising systems for biomedical applications such as drug delivery (Vallet-Regí et al., 2011). Mesoporous hybrid materials can host and interact with different drugs (Ilhan-Ayisigi & Yesil-Celiktas, 2018), including Tenofovir (TFV) as previously reported (Martin-Illana et al., 2020).

The possible interaction between components in a pharmaceutical formulation is always taken into account in terms of drug bioavailability and efficacy. Among these interactions, polyelectrolyte complexes (PECs) are formed when electrostatic interactions are established between polyelectrolytes with opposite charge (Ishihara et al., 2019). In this sense, it is widely known the ability of chitosan to form PECs due to the presence of amine functional groups in its structure and the complexation reaction is maximized at pH conditions at the vicinity of the pK_a of the counter polymers. In acidic aqueous solution, this polymer interacts with anionic polymers such as xanthan gum, whose pK_a is 3.1 (Vinchhi et al., 2021). Karaya gum and pectin are also polyanions with great potential to form PECs, being their respective pK_a avalues about 3.5 and 4.6 (Meka et al., 2017). On that basis, it could be assumed that in the proposed formulation PECs (between chitosan and the anionic polymers) could be formed in situ once the films are in contact with the acidic vaginal medium (pH = 4.2).

With this background, trilayer films intended for the vaginal administration of TFV and based on ethylcellulose, an anionic polymer (karaya gum, pectin or xanthan gum) and chitosan were developed. An inorganic drug release modulator has been also incorporated in the manufacturing of the films whose capability to host tenofovir was previously evaluated (Martin-Illana et al., 2020). The electrochemical properties of the films have been used for the first time to identify their hydration dynamics and its influence on the formation of PECs of different size. The authors hypothesize that the swelling behavior and the ionic mobility throughout the polymer network would play a crucial role in the drug release mechanism of the proposed HIV preventing vaginal films. The effect of the formation of polyelectrolyte complexes in the polymer hydration dynamics is thus deserved to be studied by novel approaches.

2. Materials and methods

2.1. Materials

2.1.1. Manufacturing of the films

Karaya gum (LOT SLBP5629V, Sigma Aldrich, St. Louis, MO, USA, 9500 *kDa*), pectin from citrus peel (galacturonic acid >74%, LOT SLBN9007V, Sigma Aldrich, 219 *kDa*), xanthan gum (LOT SLBN1080V, Sigma Aldrich, 933 *kDa*) and chitosan (viscosity 37 mPa·S, degree of *N*-deacetylation 54.7 ± 4.2% (Cazorla-Luna et al., 2019), LOT 0055790, Guinama S.L.U., Valencia, Spain, 32 *kDa*) were used as film-forming biopolymers. Ethylcellulose (viscosity 46 cP, LOT MKBS4864V, Sigma Aldrich) was another film-forming polymer also used as polymeric drug release regulator. Glycerol (LOT 0000539368, Panreac, Barcelona, Spain) and tributyl citrate (TBC, LOT BCBP4709V, Sigma Aldrich) were used as plasticizers. Methanol (for analysis, Panreac) was used as solvent. Citric acid (LOT BCBV9045, Sigma Aldrich) was used for obtaining suitable chitosan-based films.

2.1.2. Synthesis of the inorganic drug release regulators

Triethoxysilane (TrEOS, ABCR, Germany), polydimethyl siloxane (PDMS, ABCR, Germany), isopropanol (iPrOH, Sigma Aldrich, 98%), hydrochloric acid (HCl, Fluka, 32%).

TFV (LOT FT104801505, Carbosynth Limited, Berkshire, UK) was used as antiviral drug. In the cases where it was needed, H_2O was doubly deionized (Panreac).

2.2. Methods

2.2.1. Film manufacture

The film manufacturing was carried out by the solvent casting method onto silicone well trays. The composition of the different systems is displayed in Supplementary Material S1. The monolayer films (coded C, P, X, K and E) and bilayer films (coded EP, EX and EK) were obtained by casting the corresponding solutions of the plasticizers into the silicone molds where the solids were previously poured and, after manually mixing, letting dry at RT until complete evaporation of the solvents (96 h for C films and 72 h for the remainder polymer films). For the manufacture of the trilayer films (coded CEP, CEX and CEK), the bilayer films and the monolayer C film were put together (with the layer based on the anionic polymer of the bilayer film in contact with the chitosan-based film) and subjected to a constant pressure of 10 N for 5 min. The mean thickness of the obtained films is also recorded in Supplementary Material S1. Thickness was determined with a high precision vernier caliper. A schematic illustration of the manufacturing procedure is shown in Supplementary Material S2a. All films were individually prepared at their final size, with polymers and drug being precisely weighed for each film.

2.2.2. Inorganic drug release regulator synthesis

The inorganic drug release regulators were synthesized by the sol-gel method and subsequently loaded with the drug following the procedure described by Martin-Illana et al. (2020). In brief, TrEOS and PDMS were placed in a flask heated at 70 °C and maintained under reflux (weight ratio TrEOS/PDMS fixed to 2.33). iPrOH was used as a solvent and H_2O and HCl were added to promote hydrolysis and polycondensation. After 60 min reaction, the sols were transferred to polypropylene containers and 30 min later, NH_4OH 1 M was incorporated to promote gelling (volume ratio 2:1, sol:NH_4OH). The gels were then heat treated at 700 °C in N_2 atmosphere to obtain the inorganic porous particles used as drug release regulators. The drug was then loaded onto the particles by

immersion of 75 mg in 12 mL of a TFV solution (6.5 mg/mL) in Falcon tubes for 60 min (the time needed for achieving the maximum loading capacity of the particles as previously determined). Tubes were maintained in an oscillating water bath (P Selecta® Unitronic-OR) at room temperature and 45 opm during this time, and particles subsequently filtered and dried at 50 °C for 24 h. These inorganic drug release regulators were introduced in the trilayer films during the manufacture of the bilayer component in a percentage of 5%, 10% and 20% w/w over the total amount of polymer in the final film.

2.2.3. Swelling test

Given the ability of some hydrophilic polymers like chitosan and plant gums to uptake water and swell once they are in contact with an aqueous medium (Yadav et al., 2010), swelling test was performed to determine the influence of vaginal fluid in the films developed. Swelling studies were performed by fixing a fragment of each film ($2 \times 2\ cm^2$) to a stainless steel disc by using a cyanoacrylate adhesive. In the case of the bilayer and trilayer films, the ethylcellulose-based layer is placed facing outward thus simulating in vivo administration. The films were then immersed into 100 mL of simulated vaginal fluid (SVF, pH = 4.2) -which was prepared according to the established method (Owen & Katz, 1999)- contained in beakers that were heated at 37 °C and shaken at 15 opm in the oscillating water bath. At prefixed times, the discs with the films were extracted from the beakers and weighted after removing the excess of medium with a towel paper. The swelling ratio (*SR*) was calculated from the weight of the swollen (F_s) and dried (F_d) films according to the equation below. This assay was carried out in triplicate for each batch.

$$SR\ (\%) = \frac{F_s - F_d}{F_d} \times 100 \quad (1)$$

2.2.4. Scanning electron microscopy (SEM)

In order to determine the arrangement of the polymers in the films and the possible interaction between chitosan and the natural polymer from the bilayer component in the trilayer films, the cross-sectional microstructure of the films was observed by SEM. Images were taken in the as-prepared films and in the swollen films. These swollen samples were prepared by immersing the films in SVF during 0.5 h in the case of monolayer films and 24 h for the bilayer and trilayer films under the conditions previously described for the swelling test, followed by a freeze-drying process to dehydrate the swollen films. All the films were coated with gold prior to analysis to provide electronic conductivity using a gold sputter module. A Field Emission Scanning Electron Microscope (FE-SEM, Hitachi S4700, Tokyo, Japan) operating at 20 kV and backscattered electrons was used.

2.2.5. Electrochemical impedance spectroscopy (EIS)

EIS measurements were performed on a PGSTAT204 potentiostat/galvanostat (Metrohm Autolab, B.V., Sweden) using Swagelok® cells in a two electrode setup by using electrochemical grade stainless steel rods as current collectors and at room temperature. The films were cut and placed in the Swagelok® cell and 80 μL SVF was then added. EIS measurements were carried out in the frequency range from 0.1 to 10^5 Hz at open circuit potential and at a certain time intervals.

2.2.6. Mechanical properties

The influence of the nature of the polymers forming the films and their crosslinking structure in the mechanical resistance of the systems was established by this test. Mechanical properties (elastic modulus and maximum load) were determined in films stripes of previously measured dimensions (about 30 mm length and 6 mm width, thickness values collected in Supplementary Material S1) preloaded at 0.2 N in a tensile machine (DY 30, Adamel Lhomargy) fitted with a 10 N load cell. A constant tensile force was applied at 10 mm/min until the rupture of the film stripe. This test was performed in quadruplicate for each batch.

2.2.7. Mucoadhesion test

In order to quantify the ability of the films to remain attached to the vaginal mucosa thus increasing the permanence of the formulations in the site of administration, mucoadhesive properties of the films were determined by an ex vivo test based on a previously used methodology (Martín-Illana et al., 2019). Briefly, a TA.XTplus Texture Analyzer (Stable Micro Systems, Surrey, UK) with a 5 kg load cell and a cylinder probe of 10 mm diameter was used. A 10 × 10 mm sample of the film was adhered to the probe using double-sided tape by the ethylcellulose-based layer, thus exposing the layer mainly containing the corresponding mucoadhesive polymer to the mucosa. A piece of bovine vaginal mucosa (obtained from a local slaughterhouse) was fixed with ethyl cyanoacrylate adhesive (Loctite®) by its serosal side in the bottom of a 5 cm diameter Petri dish, which was fixed on the table of the texture analyzer. From an initial height of 30 mm, the probe moved down and compressed the film against the mucosa applying a force of 4.9 N at 0.1 mm/s after a trigger force of 0.049 N was attained. After 30 s, the probe moved up to the initial height at 0.1 mm/s, so that the film detached from the mucosa. Detachment force, which is the maximum force necessary to remove the sample from the mucosal substrate, and work of adhesion, that is defined as the area under the force-displacement curve, were evaluated. This assay repeated four times for each batch in different places distributed over the mucosa. The data obtained were statistically analyzed using Student's *t*-test (considering $p < 0.05$ was significant).

2.2.8. Drug release test

Since one of the main objectives of this work was to obtain drug-controlled release films through a hydrophobic polymer and an inorganic excipient, the role of both materials for achieving this type of release was evaluated. For the drug release experiments, three films of each batch containing the inorganic excipient were placed in borosilicate glass flasks containing 40 mL of SVF. The flasks were heated at 37 °C and shaken at 15 opm in the oscillating water bath. At prefixed times, 5 mL of each flask were collected and filtered, also replacing them with 5 mL of fresh SVF. The amount of TFV dissolved in the medium was determined by UV–vis spectroscopy (Evolution TM 60S, Thermo Scientific TM, Kyoto, Japan) at the wavelength of 261 nm corresponding to the maximum absorption of TFV.

3. Results

3.1. Swelling behavior of the mono and multilayer films

Fig. 1 shows the swelling profiles of the films during the test. In Fig. 1a, it is presented the swelling behavior of the monolayer films (notice that E film is not presented because it is a high hydrophobic polymer which results in non-swellable films) (Kaur et al., 2018). The most prominent result is the high swelling ratio (*SR*) presented by the film X, which experiments a continuous increase in size of the polymeric network due to the entry of the fluid. This high SVF uptake ability of xanthan gum-based films was previously reported (Cazorla-Luna, Notario-Perez, Martin-Illana, Bedoya, et al., 2020). Karaya gum is naturally insoluble in water and its swelling characteristics are attributed to the relative large amount of acetyl groups (Padil et al., 2018). In the case of the chitosan films, after the first moderate swelling (see at the inset in Fig. 1a), a gradual weight loss occurs because of the film dissolution in the SVF (Notario-Pérez et al., 2017). In the remainder biopolymer films after a first moderate swelling, the curves show a decrease in the *SR* caused by osmotic de-swelling. This osmotic effect drives water molecules out the film structure, causing shrinking and even polymeric chain collapsing (Saunders & Vincent, 1999).

In the bilayer and trilayer films (Fig. 1b), the presence of the E layer prevents the film from collapsing thus showing a positive *SR* during the whole swelling period against that observed in the case of K and P monolayer films. It is worth to notice that despite the positive swelling

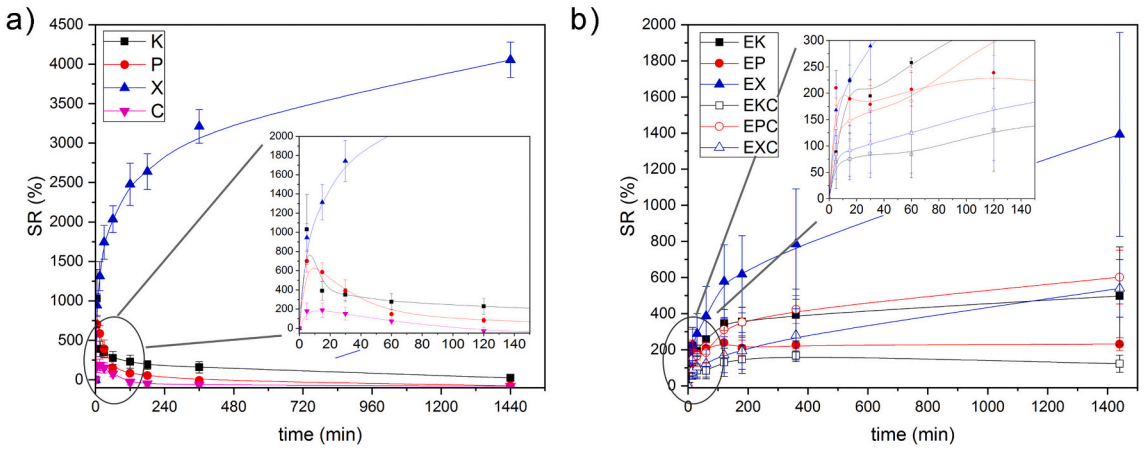

Fig. 1. Swelling behavior of a) monolayer films and b) bilayer films (solid symbols) trilayer films (open symbols). Inset shows the detail of the film swelling during the first 150 min. Notice the change of y-axis scale in figures a and b.

during the whole swelling period, both the bi and trilayer films present lower *SR* ratios than the monolayer films. Again, the films manufactured with xanthan gum present the highest *SR*, being the ones prepared with pectin and karaya gum the respective bilayer and trilayer films which are the swollen indicating that the nature of the biopolymer influences the water captured from the medium by the systems.

To better observe the microstructural changes occurring in the films during swelling, Figs. 2 and 3 show the SEM images of the films prepared with a single polymer (monolayer films, Fig. 2) and the films containing the polymeric drug release regulator and the mucoadhesion enhancer (trilayer films, Fig. 3), all of them taken before and after the swelling experiments. As observed in Fig. 2a.1 and a.2, the films K present a microstructure typical of a collapsed network. In the case of using pectin (Fig. 2b.1 and b.2), P films show an open cellular microstructure after swelling whereas the microstructure of X is more like a scaffold, which might explain its high resistance to collapse. C films, on their side, transform from a uniform and non porous microstructure to a disintegrated polymeric network. These differences in the microstructure of the monolayer films allow explaining the swelling differences related to the nature of the film-forming polymer. The high SR of X films results in the large pores observed in the microstructure after swelling while the lower swelling degree of K, P and C films produces microstructures with pores of lower size after swelling.

In the case of the bilayer films where the controlled release polymer (E) prevents from collapsing, it is clearly appreciated the two layers, especially after swelling (Fig. 3). The thin and less porous layer at the left of the images corresponds to E while the thicker porous layer at the right is formed by the corresponding swellable polymer – K, P or X -. This arrangement in two layers was previously observed in films composed by ethylcellulose and xanthan or tragacanth gum (Cazorla-Luna, Notario-Perez, Martin-Illana, Bedoya, et al., 2020). In the films EK and EP (Fig. 3a and b), large pores are observed in the swollen films

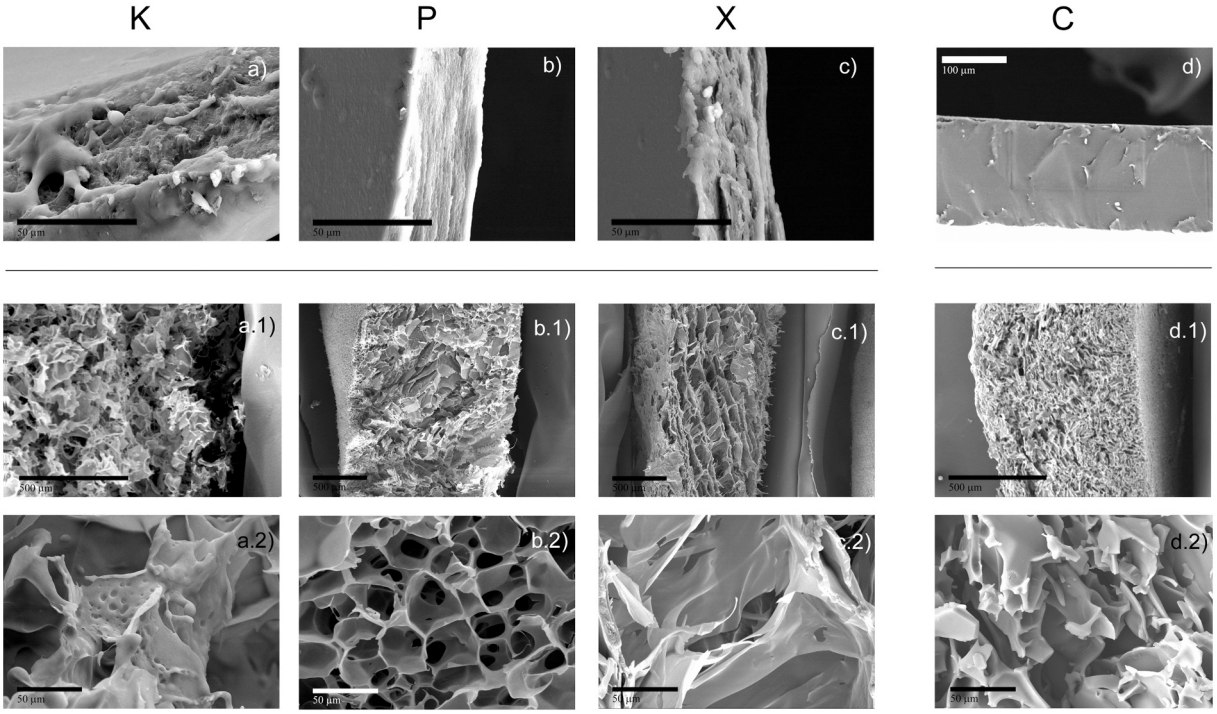

Fig. 2. SEM images of the a) – d) fresh films (scale bars are 50 μm in a-c and 100 μm in c) and X.1) X.2) freeze dried films after the swelling test (scale bars are 500 and 50 μm in panels X1 and X2, respectively). Images correspond to a) karaya gum b) pectin c) xanthan gum and d) chitosan citrate.

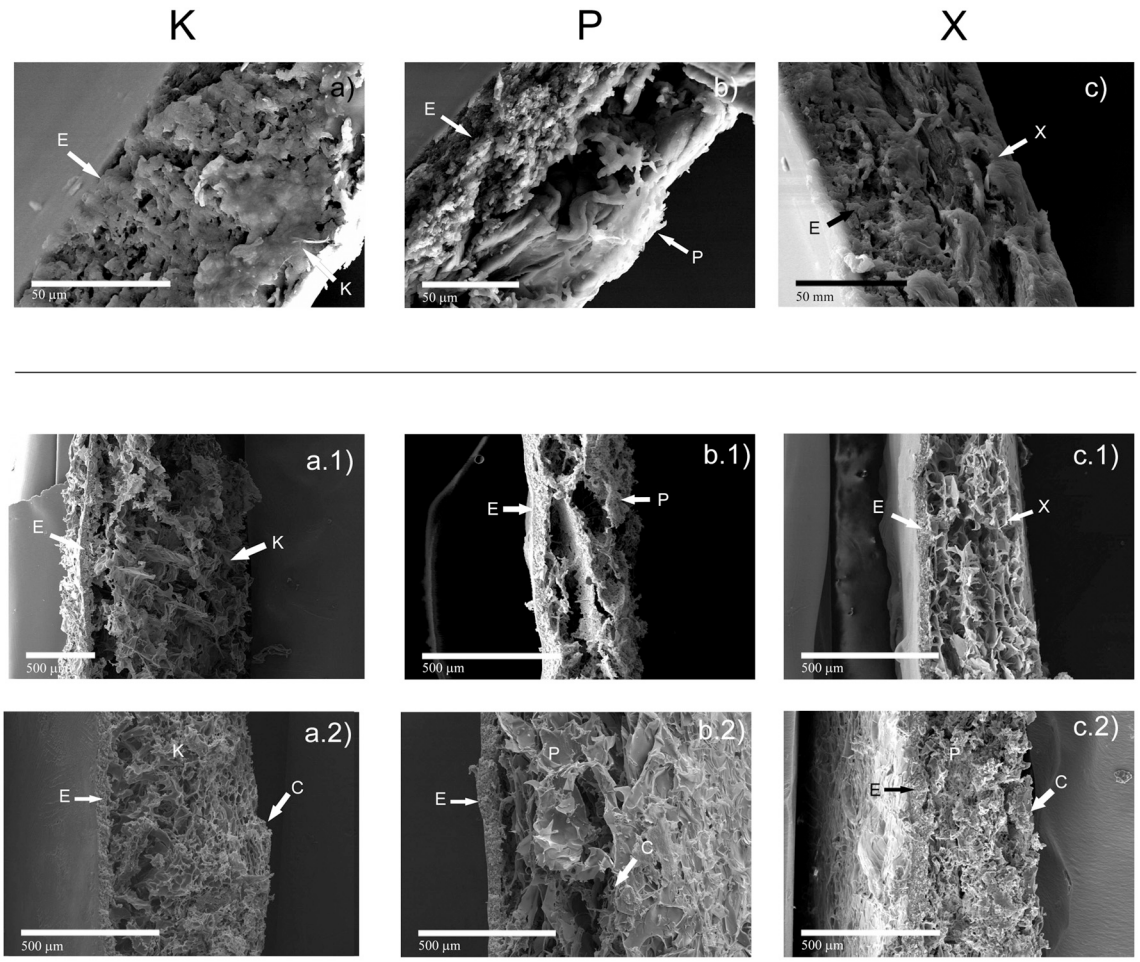

Fig. 3. SEM images to the a) – c) fresh films and a, b, c.1) freeze dried films containing the drug release regulator and a,b,c.2) freeze dried films containing the drug release regulator and mucoadhesion enhancer. Figures correspond to a) karaya gum b) pectin and c) xanthan gum. Scale bars are 500 μm in all the cases.

attributed to the biopolymeric structure which is supported by the non-swelled E layer. In the case of bilayer EX films (Fig. 3c), on contrary, the scaffold-like microstructure of X is still appreciated. The bilayer arrangement of the polymers in EK, EP and EX films allows explaining the decrease in the *SR* from monolayer to bilayer films. In the case of trilayer films, it should be highlighted that the E layer can be still differentiated at the right of the images. However, the remainder images of the cross-sectional microstructure are homogeneous in appearance not allowing distinguishing the chitosan-based layer.

3.2. Effect of the film components on the penetrability of the SVF

Hydration dynamics of water-penetrating pastes has been studied by impedance spectroscopy techniques for a long time (Christensen et al., 1994; Dotelli and Mari, 2001). EIS study was therefore performed to determine the conductivity profile of the films as a tool to understand the fluid penetrability and mobility of SVF into the polymeric matrices. In all the cases, the ionic conductivity was derived from the EIS curve by using Eq. (2)

$$\sigma = \frac{t}{S\,R_{ct}} \tag{2}$$

where t is the thickness of the film, S is the electrode surface (28.3 mm^2) and R_{ct} is the ohmic resistance taken at the intersection between the semicircle of the Nyquist plot and the real axis. R_{ct} was calculated by fitting the EIS curve to an electrochemical circuit, as it will be described in the following sections.

3.2.1. Effect of the polymer on the conductivity of the SVF

Each of the monolayer films were subjected to a first impedance spectroscopy characterization collecting the spectra at different time intervals in order to identify the changes occurring in these polymers when they are in contact with the SVF. In a typical EIS spectrum as a function of frequency, three domains can be found: (i) low frequency dependent domain, (ii) medium frequency plateau, and (iii) high frequency dependent domain. In Fig. 4a, it can be appreciated the different behaviors depending on the chemical nature of the polymers. The Bode plots showed in this Fig. 4a, present two well differentiated regions. At low frequency regions, the behavior of all the biopolymers is predominantly capacitive attributed to the formation of a double layered configuration where the inner part of this structure is filled with the SVF. The closer is the phase angle to −90°, the higher the capacitive response. Then, at high frequency regions, the phase angle collapses to zero at different velocities according to the polymeric structure indicating different transitions towards the resistive behavior.

Both K and P films are strongly modified in the presence of the SVF with an increase of the frequency region at which the capacitive to the resistive behavior takes place with time. X, on contrary, shows almost no variation of the Bode plots with time, probably because of the high viscosity of the gel formed by this biopolymer. The opposite occurs in the case of the chitosan film where at a certain frequency (around 10^3 Hz) there is a change in the slope of the curve in the Bode plot indicating a frequency-dependent event (charge transfer) that becomes minimized as the SVF penetrates into the film.

From the intersection of the semicircle formed in the Nyquist plot

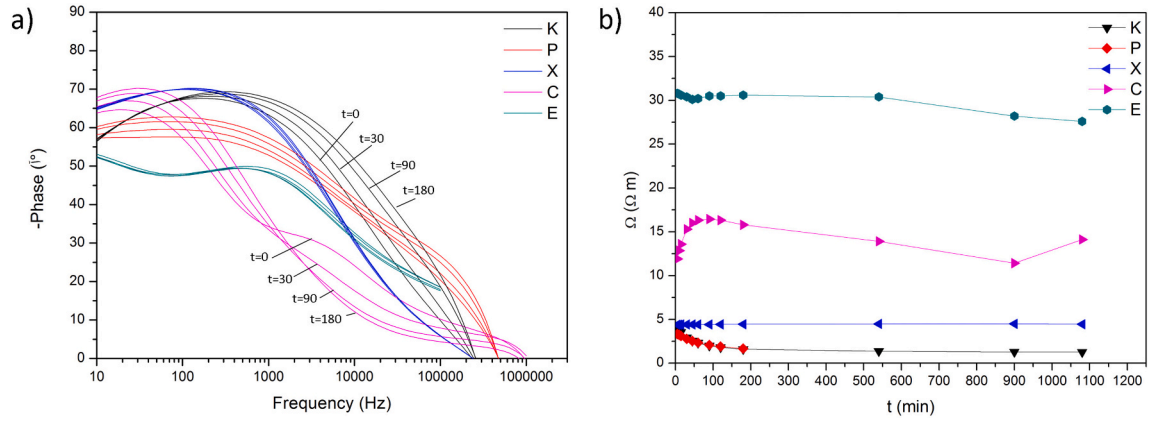

Fig. 4. a) Bode plots of the films prepared with a single polymer (monolayer films) determined at different soaking times and b) Evolution of the resistivity of the films as a function of the soaking time.

(shown in Supplementary Material S3) with the real axis (Z′ vs Z″), the resistance of the films can be calculated (Fig. 4b). The electrochemical circuits used to fit the EIS curves and to obtain these resistance values are provided in Supplementary Material S4. Due to the low wettability of the ethylcellulose, the film labeled E presents the highest ohmic resistance followed by the film prepared with chitosan that presents an increase in the resistivity of the film during the first 100 min soaking and then it is maintained constant. In the case of the films manufactured with pectin and karaya gum, their resistivity decreases progressively during the first 180 min soaking and afterwards remains more or less constant. In the case of the P film, it was not possible to determine the resistance of the film at high soaking periods because it disintegrated. No differences in the conductivity during the whole soaking period were observed in the film containing xanthan gum, which shows slightly higher values than P and K films.

Additional information about the fluid penetration into the prepared films can be obtained from the calculation of the dissipation factor. The ratio of mobile and stored dipoles is defined as the dissipation factor (tan δ), which is the property defined as the electrical property proportional to the ratio between the conductivity of the polymer to its capacitive reactance at a specified frequency. During the application of the electric field, several possible mechanisms can be used to explain the behavior of the current: electrode polarization, orientational polarization, space charge effects, tunnelling of charge from the electrodes to empty traps, and hopping of charge carriers through localized states and it is related with the formation of charged complexes. In this case, the dissipation factor profile also provides information about the polymer relaxation (Capaccioli et al., 2000; Yu et al., 2008). In Fig. 5a and b, it is observed an increase of the dissipation factor in the films produced with karaya gum and pectin as the soaking time increases. During hydration the dissipation factor peak increases in its frequency and intensity indicative of an increased concentration and strength of the oscillating dipole relaxation. The quasi-identical dissipation profile with time observed in the films X (Fig. 5c) indicates that despite the high fluid penetrability, there is no variation in the number of mobile dipoles, i.e. a constant conductivity value probably attributed to the high viscosity of the gel. In

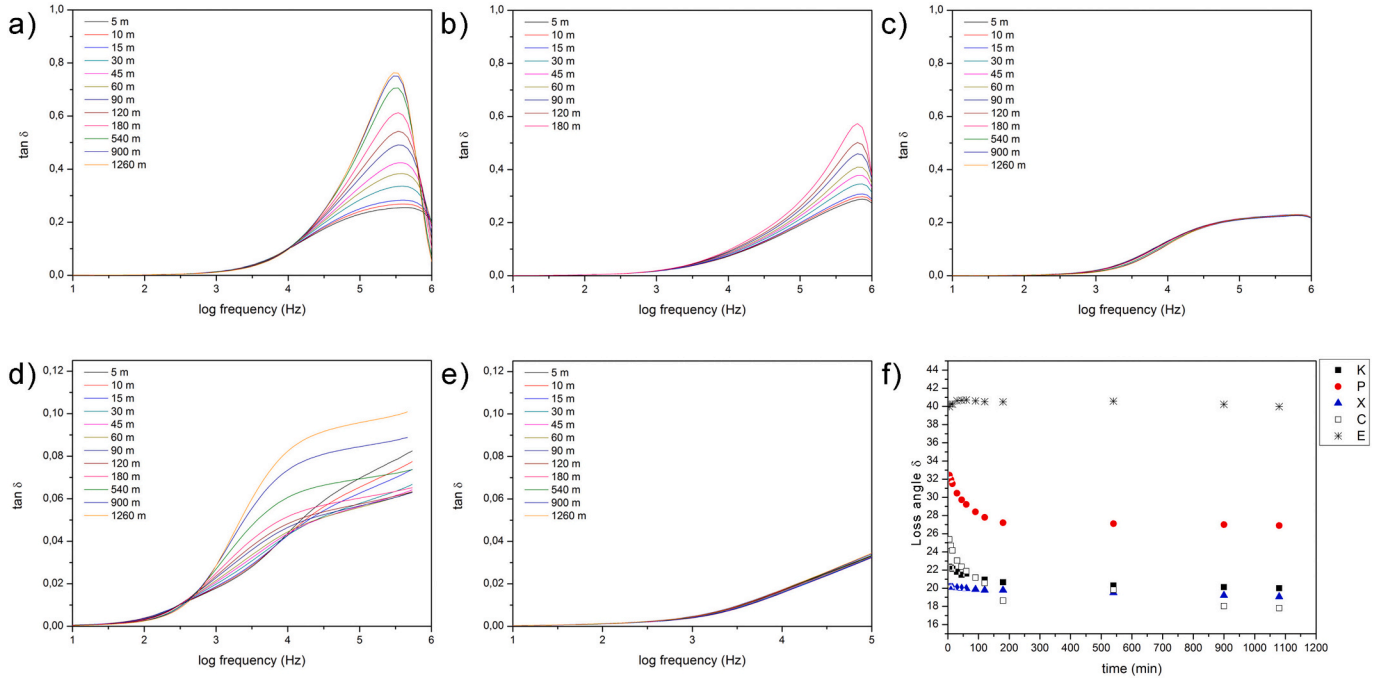

Fig. 5. Dissipation factor as a function of the frequency collected at different soaking times in obtained for the polymers a) karaya gum, b) pectin, c) xanthan gum, d) chitosan and e) ethylcellulose and f) value of the loss angle corresponding to the maximum of tan δ.

the case of the C film, we cannot find a clear maximum of the tan δ but in general, at high frequency values, it occurs firstly a decrease of the dissipation factor but then, after a certain time, this value starts to increase. Basically, there is a competition between two different relaxation processes at medium and high frequencies, whereas the high frequency relaxation vanishes with soaking time, the medium frequency relaxation increases and becomes predominant after 90 min (see also Fig. 4). The described behavior is attributed to the disintegration or dissolution of the film when in contact with the SVF and it is in agreement with the observed fall of the charge transfer events occurring in this polymer with time and shown in Fig. 4b (Notario-Pérez et al., 2017). In Fig. 5e, the values of the dissipation factor of the films E remain constant with time because of the high hydrophobicity of the ethylcellulose polymer (Cazorla-Luna, Notario-Perez, Martin-Illana, Bedoya, et al., 2020).

From the maxima of the dissipation factor curves we have calculated the loss angles whose variation with time is used in the present work to understand the ability of the film components to align their dipoles upon the presence of the electric field and the ions in the SVF (Fig. 5f). These results imply different hydration mechanisms of the individual polymers. The high hydrophobicity of E film leads to the highest loss angle values experiencing a slight increase during the first 30 min in contact with the SVF. In the case of P film, the loss angle decreases rapidly during the first 200 min suggesting a fast and homogeneous penetration of the SVF into the polymeric chains thus allowing the dipoles to be oriented in the direction of the electric field. The C film also experiments a fast hydration in the first 60 min experiment, even faster than P film. Pectin and chitosan are the most soluble polymers and the rapid decrease of the loss angle during the first 200 min is attributed to the fast SVF penetration inside the polymeric structure. Afterwards, the loss angle remains constant suggesting the formation of an electric double layer at the polymer interface. On their side, the decrease in the loss angle is minimal in the case of the K film and more especially in X films, a fact that is attributed to the high connectivity of the polymeric chains and the high viscosity of the resulting solution which difficult the occurrence of multiple charge transfers. All these results imply that there are multiple wetting mechanism depending on the physic chemical characteristics of the polymer.

3.2.2. *Influence of the polymeric mucoadhesion enhancer and drug release regulator on the fluid mobility*

Fig. 6 shows the resistivity values obtained from the fitting of the Nyquist plots (Supplementary Material S3) to the corresponding electrochemical circuits (Supplementary Material S4). Fig. 6a represents the resistance to the mobility of the SVF when in direct contact with the layer based on the natural biopolymers karaya gum, pectin or xanthan gum of the bilayer films. The bilayer samples EX exhibit 20 times higher resistivity than the corresponding monolayer films although the resistivity of EX experience a decrease with soaking time and at the end of the experiment, the conductivity value exceeds 12 times the value of the X film. Moreover, contrary to that occurred in the monolayer films, the presence of the drug release regulator E film leads to a first increase of the resistivity values during the first 45 min soaking and then decrease. This increase in the resistivity is more pronounced in the case of the films containing karaya gum, being the resistivity of EK bilayer of ~90 times (~138 Ω) than K film at time 0, increasing until ~115 times (~170 Ω) after 40 min of soaking and then decreasing to a value 55 times higher (~82 Ω) than the values obtained for K. Notice that the film E (Fig. 4b) presents the highest resistivity values among the monolayer

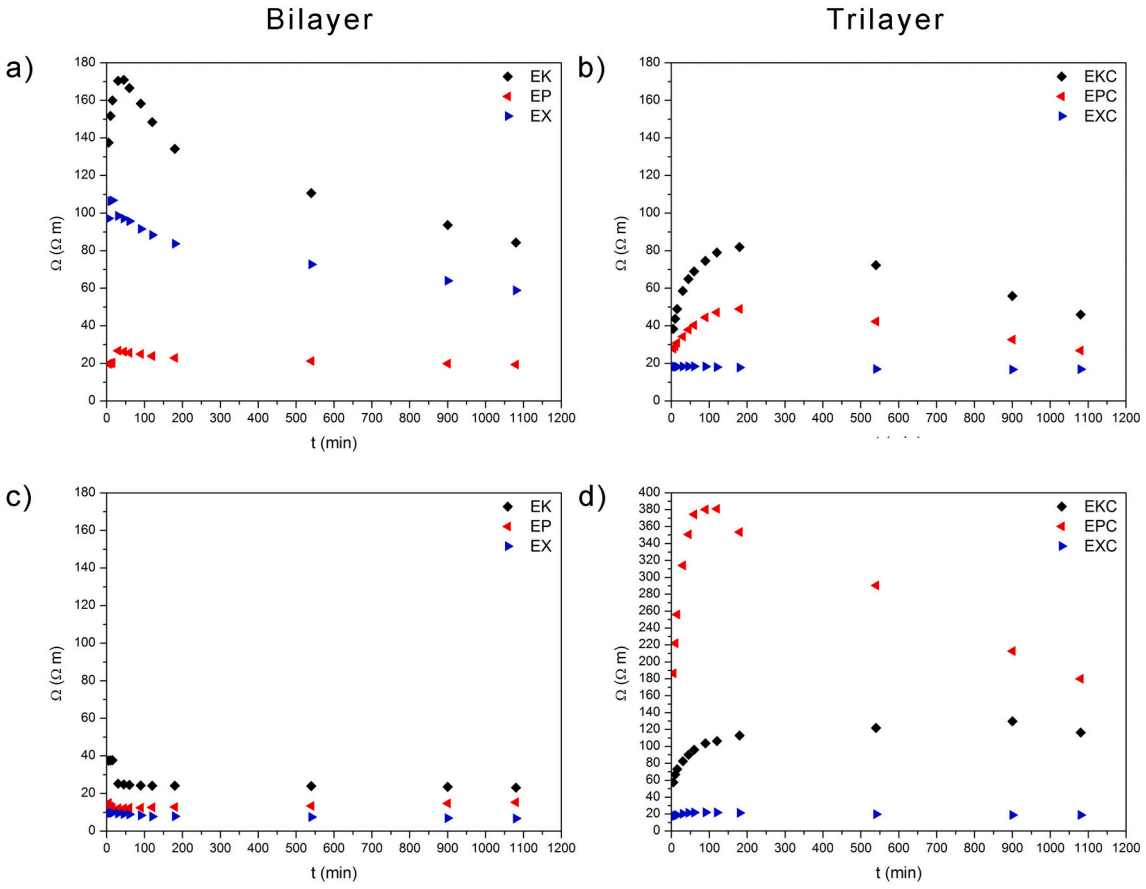

Fig. 6. Evolution of the resistivity of the films as a function of the soaking time a) bilayer films where the SVF is in direct contact with the polymer b) trilayer films where the SVF is in direct contact with the mucoadhesion enhancer layer c) bilayer and d) trilayer films where the SVF is in direct contact with the drug release regulator.

films (~30 Ω) so, it can be deduced here that the penetration of the fluid is affected, probably by the path that the electrical field must follow through the joint between natural biopolymer (P, X and K) and the drug release regulator E film.

It is worth to notice the dramatic decrease in the resistivity values of the bilayer films where the SVF is in direct contact with the polymeric drug release regulator layer (Fig. 6c). Considering the high hydrophobicity of E film, in Fig. 6a, it should be taken into account that the E layer will help the polymer wettability since all the 80 μL of SVF will exclusively interact with the K, P or X polymeric chains but not with the E layer, from where it is repelled. Here, the resistivity values show a similar trend to the monolayer films in the sense that there is a continuous decrease in the resistivity due to the fluid penetrability through the layer containing the biopolymers karaya gum, pectin or xanthan gum.

Trilayer films where the SVF is in contact with the drug release regulator E (appropriate configuration in in vivo administration) shows that EPC sample presents the highest resistivity and is highly influenced by the presence of all the components of the trilayer structure (Fig. 6d). EPC film experiments a high increase in the resistivity at the very first minutes after soaking and afterwards decrease while the remainder soaking period. In the case of the trilayer EKC and EXC films, the increase of the resistivity during the first minutes is less pronounced and more sustained and both films tend to reach similar resistivity values at the end of the experiment.

It is known that karaya gum interacts via reversible electrostatic interactions with chitosan to form PECs (Ramakrishnan et al., 2021),

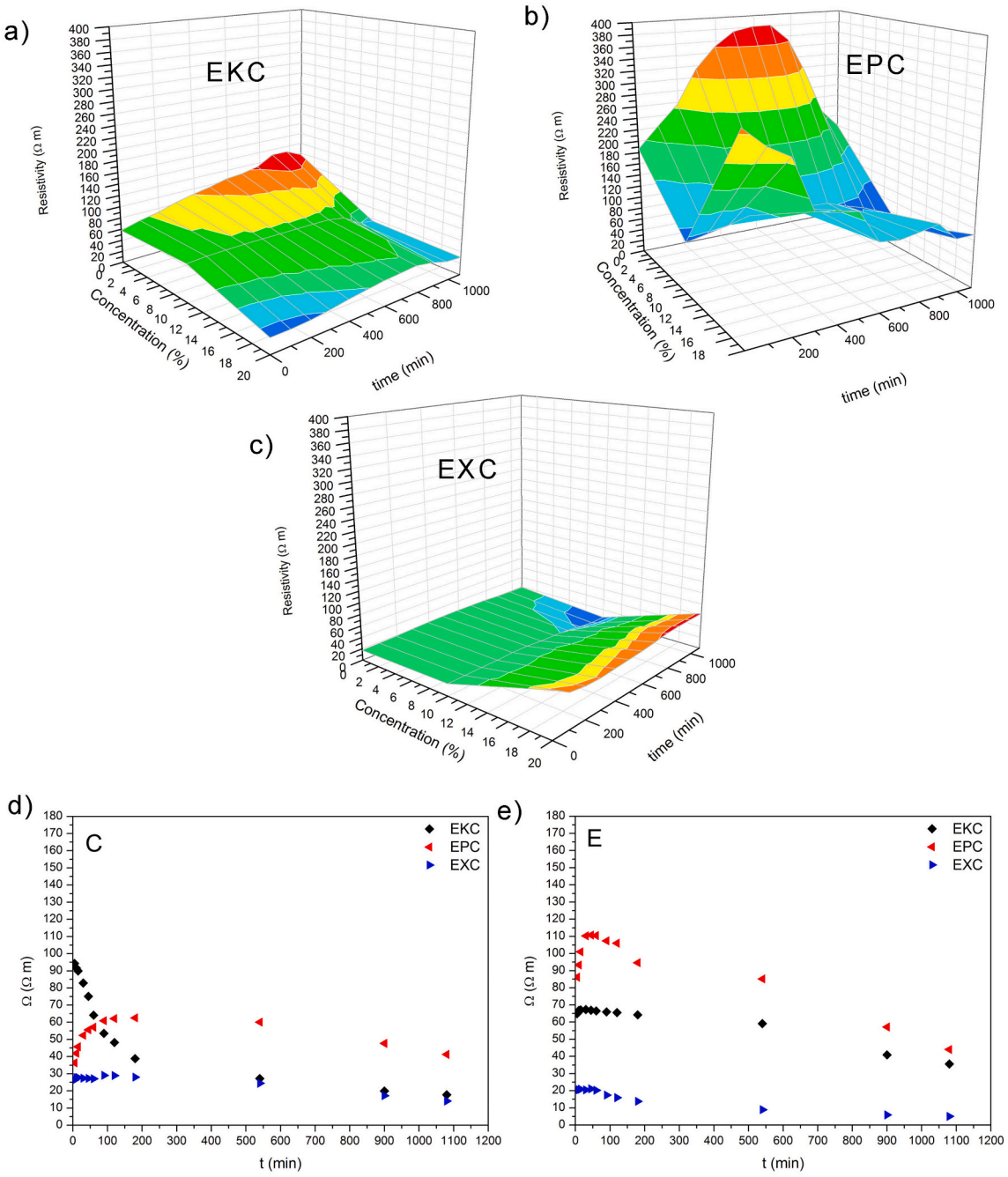

Fig. 7. Resistivity values of the trilayered films a) EKC, b) EPC and d) EXC filled with different inorganic drug release regulators where the exposed layer to the SVF contains the organic drug release regulator. Resistivity values of the trilayer films manufactured with 10% particles and where the SVF is primarily in contact with d) mucoadhesion enhancer citrate layer and e) drug release regulator.

which are defined as macromolecular materials containing repeating units capable of dissociate into highly charged polymeric molecules upon being placed in any ionizing solvent thus forming either a positively or negatively charged polymeric chain (Lankalapalli & Kolapalli, 2009). In both cases, bilayer and trilayer films (except when the SVF is in contact with E in the trilayer films), the materials containing the polymer karaya gum present the higher resistivity, i.e. it is less ionic conducting, suggesting that despite the SVF penetrates into the film, there exists a K-E interface that difficult the ionic mobility within the polymeric chains. Additionally, and contrary to that occurs in the remainder polymers, both the bilayer and trilayer containing karaya gum suffer from different wetting mechanism after the first 30 min soaking, a result that can be deduced from the change in the shape of the EIS curve and, consequently, the electrochemical circuit that fits best to the curve (see Supplementary Materials S3 and S4). In the case of the polymer xanthan gum, however, the presence of the C favors the ionic mobility thus provoking a general decrease in the resistivity values with respect to the bilayer films when the SVF is in contact with the biopolymer layer.

3.2.3. Influence of inorganic drug release regulators on the fluid mobility

Trilayer films were also manufactured with different concentrations (5, 10 and 20% over the total amount of polymer in the film) of an inorganic drug release regulator and the measured resistivity informs on the effect of the particles on the wettability of the films and the charge mobility, directly related with the PECs formation. The conductivity of the all the prepared films experiments a general decrease when C is in contact with the SVF, and also decreases with the increase of the particle content, a result that is attributed to the adsorption of the SVF by the inorganic particles. As shown in Fig. 7a, the films manufactured with the polymer karaya gum (EKC films) are positively influenced by the incorporation of the particles in the sense that large particle concentration produces a decrease in the resistivity, i.e. the larger ionic conductivity of the film. The contrary occurs in the case of the film EPC. The films with no particles added already presented high resistivity. The incorporation of 10% particles enhances the wettability of the film, a result that is deduced from their reduced resistivity. However, the particles are not always beneficial since incorporating 20% particles acts in detrimental of its conductivity, probably because of the water adsorption of the particles. In the case of EXC film, it is clear an increase of the resistivity with the incorporation of the particles, and the more particles are present, the highest is the resistivity, i.e. the lowest is the conductivity of the films because of a decreased film wettability capability.

For a better visualization of the effect of the particles in the films, we are focusing our attention in those produced with 10% particles (Fig. 7d and e). As previously commented, all the films are influenced by the incorporation of the particles: particle-free EXC films already presented quite good ionic mobility (low ionic resistivity) and as observed in Fig. 7e, even in the case that the SVF is in contact with the mucoadhesion enhancer, the resistivity of the film remains lower than in the remainder polymers. In EXC films, there is a minimum increase in the resistivity values collected at a certain time of the film manufactured with the inorganic modulator with respect to the films produced in its absence (Fig. 7d and Fig. 6d, respectively). It is also appreciated that the decrease in the resistivity with soaking time is more pronounced in the presence of the particles, a result that suggests that the particles could benefit the mobility of SVF inside the film. This effect is even more pronounced when the SVF is in direct contact with the mucoadhesion enhancer (Fig. 7e), where the resistivity values decrease from about 28 Ωm to 15 Ωm in the presence of the particles and the observed decrease is only 3 Ωm in the case of the films manufactured without the inorganic drug release modulator. The same occurs in the case of the EKC films, where the observed decrease in the resistivity as a function of the soaking time implies that despite of the poor conductivity, the particles might enhance the ionic mobility of the SVF.

EPC is the film which experiments the highest increase in the resistivity values at low soaking times because of the incorporation of the particles, even at such concentration (as commented before, the highest increase was found for the 20% inorganic regulator concentration) but then starts to decrease. This decrease in the resistivity is more pronounced when the SVF is in contact with the drug release regulator E indicating a faster water penetration (despite the high hydrophobicity of E). Nevertheless, the variation in the resistivity is less pronounced than in the case of the films manufactured in the absence of the particles (Fig. 6d) suggesting that in spite of the good predisposition of the EPC films to be wetted, the presence of the particles somehow hinders the ionic mobility.

3.3. Mechanical properties of the trilayer films

The Young Modulus and maximum resistance (*Rm*) of the films has been calculated from the load-extension curves obtained in the elongation test (given in the Supplementary Material S5). In Fig. 8 it is observed that the mechanical properties of the monolayer films synthetized using karaya gum biopolymer are quite compromised, both in the young modulus and the *Rm* whereas the films P are the one presenting the better mechanical properties. When the bilayer and trilayer films are tested, the films containing pectin are the ones showing the poorest mechanical properties, a result that is attributed to the different elastic behavior of P and E films (Fig. 8a). On contrary, in the films manufactured with karaya gum, the similar mechanical properties found in the two polymers alone exert a synergistic behavior in the multilayered films thus presenting the best mechanical properties in terms of the Young Modulus and *Rm*. Finally, combining E and X films, both parameters show intermediate values between those of the corresponding polymers separately.

3.4. Mucoadhesive properties of the films

An *ex-vivo* test was used to assess the mucoadhesion of the trilayer films to the bovine vaginal mucosa. Due to the poor mechanical properties of the films containing the polymer pectin, only the films prepared with K and X films were evaluated. Mucoadhesion is defined as the interaction force between the mucin surface and a synthetic or natural polymer. There, it should be noticed that all the films have been tested facing the chitosan-based mucoadhesion layer towards the mucosa as expected during in vivo administration. The work of mucoadhesion is more appropriate to describe the mucoadhesive properties of the films as it can be used as a parameter indicating the stickiness of the formulation. It is related to the surface tension of the C layer and the substrate, i.e. the vaginal mucosa (Bassi da Silva et al., 2018). As previously reported, the mucoadhesiveness of the chitosan polymer is dominated by electrostatic interactions (Cazorla-Luna et al., 2019; Czechowska-Biskup et al., 2012). The calculation of the mucoadhesion force of the trilayer EKC and EXC film is shown in Supplementary Material S5. The paired *t*-test carried out in these results revealed that there are minimal differences in the mucoadhesion of the two tested trilayer films falling these variations within the systematic error.

The averaged value for the work of mucoadhesion (also recorded in Supplementary Material S5) is about 0.5 N.mm, similar to the values obtained by Cazorla-Luna et al. in chitosan-based vaginal tablets (Cazorla-Luna et al., 2019) and in the range of the data resulting from films comparable to those developed in this work (Cazorla-Luna, Notario-Perez, Martin-Illana, Bedoya, et al., 2020). Again, the *t*-student test carried out in these data revealed that there are not significant differences between polymers and inorganic modulator content, indicating that the mucoadhesive properties of the C layer were not affected because of the presence of the two other layers in in the tested films.

3.5. Kinetics of the drug release

The influence of the drug release regulators has been studied in two cases: In the first case, the drug has been included into the

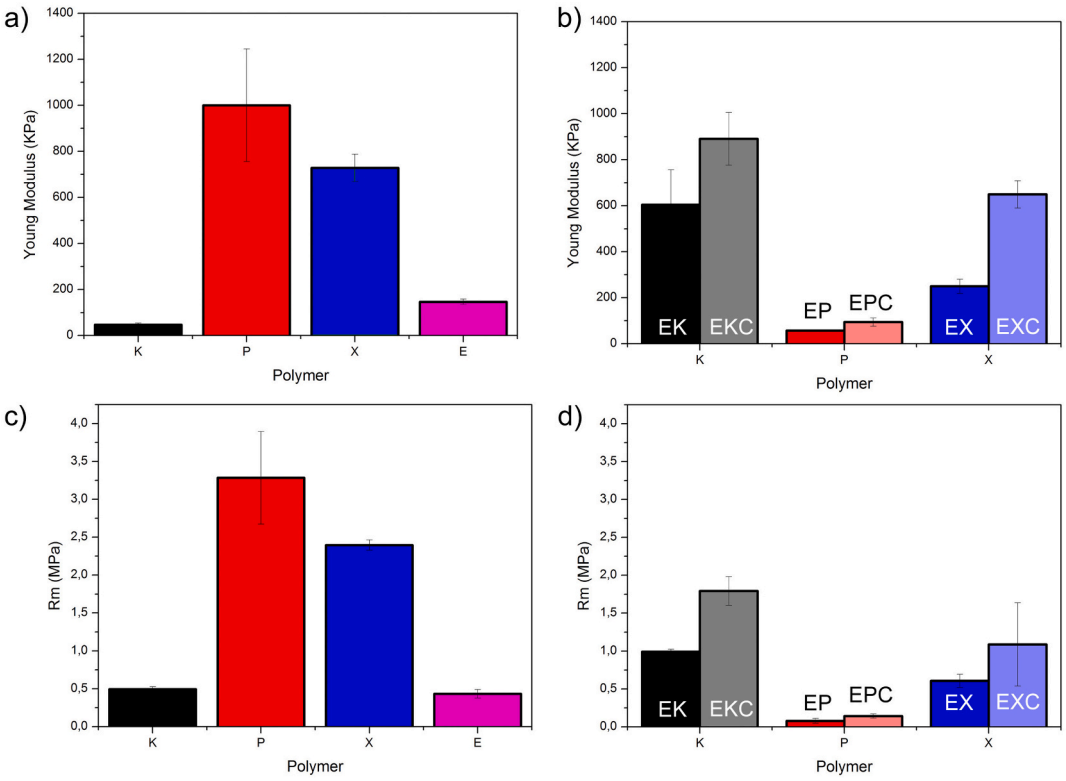

Fig. 8. Mechanical properties of the prepared films. Young modulus of a) films containing the single polymers and b) films containing the organic drug release regulator (in dark color) plus the mucoadhesion enhancer (light color). Maximum resistance of a) films containing the single polymers and b) films containing the organic drug release regulator (in dark color) plus the mucoadhesion enhancer (light color).

pharmaceutical formulation containing the organic and the inorganic modulators and, in the second case, the drug TFV has been previously loaded into the inorganic regulator. The drug release profiles have been represented in Fig. 9a) and b) respectively (notice that releasing time has been represented in the logarithmic scale for better data visualization). As it has been commented before, the technological application of the EPC formulation is quite compromised because of its poor mechanical properties so, the drug release experiments have been carried out exclusively in the two formulations that could be used in real application, i.e. those containing the karaya and the xanthan gum biopolymers. As it can be seen in Fig. 9a, there are minor differences in the drug release profiles of EKC and EXC and the release occurs slightly faster in the case of the EXC film. When the TFV was loaded inside the particles, the differences between the two polymers are more clearly seen, with a faster release profile in the case of the films containing the polymer karaya gum (Fig. 9b).

The drug release profiles have been adjusted to the most common drug release models (Tamayo et al., 2017) by using a non-linear fitting method. The two models showing the better fits (according to the Chi-square and r-square criterion) are the *First Order* kinetic model and the Weibull kinetic model. In the *First Order* model, the release rate is only dependent on the concentration of the drug whereas the parameters *a* and *b* in the Weibull model describe the drug release dependence with time in the case of *a*, and *b* takes different values as a function of the shape of the dissolution curves (Dash et al., 2010). Table 1 collects the kinetic parameters of the drug dissolution curves shown in Fig. 9 obtained from the application of the above mentioned drug kinetic release models. From the application of the first order kinetic model, the *k* parameter (kinetic constant) is higher in the case the drug is physically mixed with the polymers indicating that, effectively, the inorganic drug

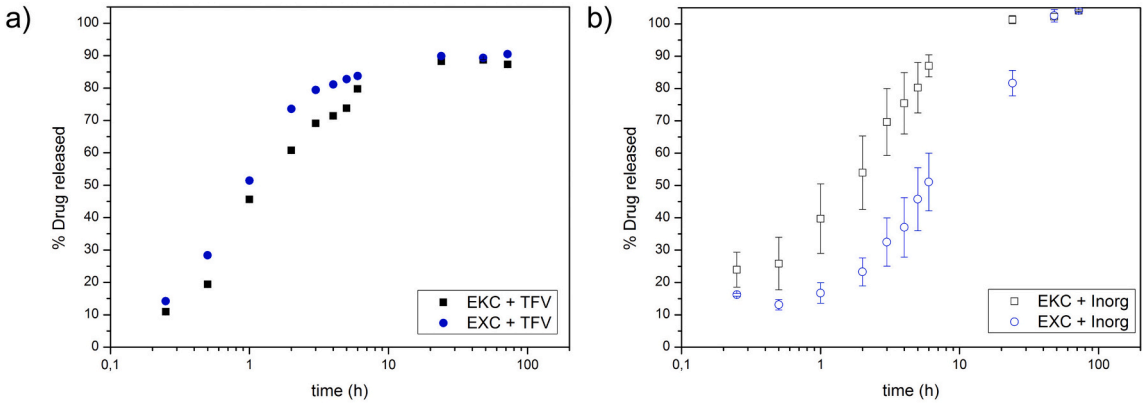

Fig. 9. Drug release profiles of the pharmaceutical formulations EKC and EXC plus the inorganic modulator where a) the drug TFV has been physically mixed with the polymers (notice the small size of error bars) and b) the drug has been previously loaded into the particles.

Table 1
Kinetic parameters of the drug dissolution curves obtained from the application of the first order kinetic model and the Weibull model.

	First order			Weibull			
	k	r^2	χ^2	b	a	r^2	χ^2
EKC + TFV	0.590	0.981	0.415	0.840	1.670	0.985	0.338
EXC + TFV	0.832	0.993	0.152	1.015	1.19	0.993	0.169
EKC + inorg	0.401	0.965	3.67 10^{-3}	0.681	1.974	0.994	5.85 10^{-4}
EXC + inorg	0.123	0.963	4.04 10^{-3}	0.623	5.698	0.988	1.22 10^{-3}

release modulator slow down the drug release and the effect is larger in the case of the X polymer than in the films produced with K. When the two polymers are compared, it is noticed that when the drug is loaded in the inorganic drug release modulator, the release occurs faster in the EKC film than in the EXC whereas the opposite behavior is found if the drug is just dispersed in the organic matrix.

Upon the application of Monte Carlo simulations, Papadopoulou et al. (2006) correlated the *b* exponent in the Weibull function with the mechanism of transport of a drug through the polymer matrix. The term *b* is expected to be proportional to the surface area of the matrix since a high specific surface means that there are more diffusion paths (Kosmidis et al., 2003). When applying the Weibull release model and concerning the diffusional mechanism, the *b* parameter indicates that the main differences between polymers are found in the case that the drug is physically mixed with the polymers. It is known that *b* values comprised between 0.75 and 1 indicate diffusion in the tridimensional matrix in contribution with another release mechanism (Papadopoulou et al., 2006). The higher is the *b* value, the more it is approached to Fick's law diffusion. According to the obtained *b* values in the EKC or EXC films plus the inorganic modulator, the diffusion of the drug occurs in a fractal or disordered substrate different from the percolation cluster (Kosmidis et al., 2003).

The *a* parameter in the Weibull's model denotes a scale parameter that describes the time dependence and, in the case of $b = 1$, it may adopt the formulae $k = 1/a$, where *k* is the kinetic constant (Dash et al., 2010). The lowest is the *a* value, the faster is the diffusion. According to this, it can be affirmed that the diffusion of TFV is slower when the drug is loaded in the particles, especially in the case of films based on xanthan gum.

4. Discussion

The comprehension of the swelling behavior and SVF penetration dynamics of the vaginal films is important from both the practical and the theoretical points of view. The swelling results bring to light the influence of the nature of the polymer in the film hydration dynamics. Hydrophilic polymers tend to swell rather than disintegrate when in contact with an aqueous medium usually experiencing a first swelling event prior to erosion or dissolution. According to Munday and Cox (2000) karaya gum owns lower water uptake capacity and greater erosion rate than xanthan gum. By their part, pectin-based films swell and then dissolve in aqueous medium (Murata et al., 2019) and chitosan citrate films rapidly dissolve in SVF as it was previously proven (Cazorla-Luna, Martin-Illana, Notario-Perez, Miguel Bedoya, et al., 2020). These behaviors allow explaining the results obtained from the swelling test of monolayer films. The addition of ethylcellulose as polymeric drug release regulator permits limiting the swelling of the biopolymers in the bilayer films due to its great hydrophobicity and also, this swelling might be limited because of the formation of the PECs with the chitosan polymer.

In the swelling test, it is clear that the *SR* is lower in the bilayer and trilayer films than in the monolayer films, although care should be taken when interpreting the results. The E layer is not able to absorb water and it does not gel either but it takes part of the multilayer films and its weight is taken into account when calculating the *SR*. Having 50% of a non-swellable layer implies that the swellable polymer could absorb the same amount of SVF as if it were the monolayer film, but the *SR* would result 50% of the actual value. With this consideration, the SEM images shown in Figs. 2 and 3 allow explaining the effect of the non swellable layer (E layer) and its importance in maintaining the structure of the films and the prevention of collapsing.

As Munday reported (Munday & Cox, 2000), in the monolayer films fabricated with karaya gum, erosion dominates the hydration mechanism, although it is noteworthy the low *SR* encountered after the incorporation of the mucoadhesion enhancer. All the studied polysaccharide gums possess several functionalities such as hydroxyl, ether, acetyl, carboxyl or carbonyl groups which are able to form PECs between the polymeric chains and the other polyelectrolytes. In addition, the excess of hydroxyl groups favors the formation of hydrogen bonds with H_2O molecules and also in form of intra and intermolecular conformations. In the case of EKC films, the swelling results suggest that the entry of water from the medium would be reduced due to the greater resistance to the water uptake because of the electrostatic interactions established when PECs between karaya gum and chitosan are formed (Cazorla-Luna et al., 2021).

EIS studies carried out in polymeric films for vaginal drug delivery in vagina show that the semicircle in the Nyquist plots became smaller by increasing the swelling time, which indicates a decrease of the film resistance and a variable distribution of the dipoles with time (Wu & Li, 2020). In the case of the bilayer and trilayer films containing karaya gum, there occurs a first increase in these semicircles (high resistivity) and then decreases again, being these variations in the resistivity more pronounced when the EIS experiments were carried out with the SVF in contact with the K or C layer in the bi and trilayer films, respectively. When the EIS experiments are performed with SVF in direct contact with the E layer, the resistivity increases progressively and then remain constant. The analysis of the behavior of the bilayer EK samples indicate that when karaya gum contacts the SVF, it rapidly starts absorbing water and swells thus inducing a fast increase in the resistivity because of the increased thickness of the film followed to a rapid decrease in this resistivity (Fig. 6c). In the trilayer EKC films, the presence of the chitosan layer minimizes this decrease in the resistivity (Fig. 6d). This modification in the resistivity values observed in the trilayer films is again attributed to the formation of complexes between karaya gum and Chitosan. If the inorganic regulator is present, it favors the formation of the PECs, as evidenced from the fast decrease in the resistivity, from 95 Ω to 40 Ω during the first 200 min soaking.

As shown in Fig. 5f, the rapid increase in the loss angle of the films prepared with pectin indicates a fast SVF penetration despite its low capability of water absorption (similar to karaya gum). In the trilayer films (Fig. 6d), the presence of the C film (Fig. 6b) exerts a strong influence in their resistivity once again attributed to the inclination of pectin to form PECs with it via ionic bonds (Bigucci et al., 2008; Maciel et al., 2015). The polymer chitosan was also wetted more effectively than the other polymers (as shown in Fig. 5f) so, in the case of the trilayer EPC films where the SVF is in contact with the C layer, the fast wetting of both P and C polymers favors the rapid formation of the ionic complexes and thus the high increase of the resistivity at low soaking times (Fig. 6d). The PECs are stabilized by electrostatic interaction between the positively charged chitosan (NH_3^+) and negatively charged pectin (COO^-) (Bigucci et al., 2008; Maciel et al., 2015). In addition, the possibility of establishing new interactions via H bonds or van der Waals forces between the carboxylic groups of pectin and the amino groups of chitosan and OH, OCH_3 or $COOCH_3$ groups elsewhere within the polymeric chains has been also reported (Munarin et al., 2012; Ranganathan et al., 2019). These hydrogen bonds established within the structure might contribute to change the observed relaxation processes (Fig. 5f) due to an increased cooperative motion of the local chains of the pectin

polymer. However, the PECs based on chitosan and pectin would result on hindering the destructuring of pectin-based film due to the more compact structure arising from PECs formed once in contact with the aqueous medium (Cazorla-Luna et al., 2021).

The incorporation of an inorganic drug release regulator to the EPC systems acts in detrimental of the conductivity of the films, showing the highest resistivity especially at long soaking periods among all the studied materials (Fig. 7b). As commented before, EPC films present a combined swelling and dissolution process since water has a plasticizing effect on pectin leading to an increase in the free volume and a weakening of the interchain interactions being these films highly influenced by the presence of the particles (Sriamornsak et al., 2007). Similarly, as occurred in the EKC films, the cellular structure of the polymer partially collapsed and is only supported by the non-swelled E layer (Fig. 3b), suggesting the fragility of the polymeric chains upon the presence of the fluid. Accordingly, the incorporation of the inorganic modulator might help to enhance this fragility thus breaking the polymeric stability by physical forces and, as a consequence the formation of the PECs is also hindered.

In the case of xanthan gum, Ćirić et al. (2020) stated that only hydrogen bonds and ionic interactions were present in the PECs formed with chitosan. The basic structural unit of xanthan gum possesses 29 highly hydrophilic oxygen atoms, most of them being OH or COO^{-}, which can accept at least two hydrogen bonds each. This leads to a great number of sorption sites leading to a high SVF sorption capability (Kocherbitov et al., 2010). As reported by Bueno et al. (2013) fickian diffusion is the mechanism that describes the water absorption during swelling of X hydrogels, which implies that the water diffusion does not depend on the polymer chain relaxation (Bueno et al., 2013). Accordingly, the dissipation profiles in Fig. 5a show practically no variations with hydration time thus indicating a constant concentration of dipoles probably due to the high viscosity of the biopolymer (Capaccioli et al., 2000; Yu et al., 2008). Nevertheless, the contribution of the high swelling profile observed in the films manufactured with this polymer to the dipole alignment cannot be disregarded.

When the inorganic drug release modulator is present and the experiment is subjected in the natural conditions, i.e. the SVF is in contact with the organic drug release regulator (Fig. 7), the films containing xanthan gum are more affected in their conductivity values than K films. In an excess of particles (20% inorganic drug release regulator), the conductivity of EXC films are greatly reduced while in the case of EKC, it experiences a continuous increase when the concentration of particles increases.

The mechanical properties of the films throw significant inputs in view of the technological development of the films. Few studies are specifically devoted to mechanical testing methods intended for vaginal drug delivery devices (McCoy et al., 2019). The reported Young Modulus values of some vaginal films intended for drug delivery are in the range of 1.5–3 MPa (Kumar et al., 2013) whereas the films manufactured in this work barely reach 0.8–1 MPa. Stiffer films are known to present fewer adherence to the vaginal tissues than more flexible films. In this work, the attention has been focused in the study of the dry films rather than the swollen films because the mechanical properties of the obtained films are far below the encountered young modulus of the vaginal tissues, which fall in the range of 7–15 MPa (Baah-Dwomoh et al., 2016). Here, the differences in the Young modulus (stiffness) of the monolayers E and C and the one obtained in the films processed with pectin may be the responsible of the poor mechanical properties of the bi and trilayer films containing pectin thus minimizing the potential of the EPC films as candidates for vaginal drug delivery systems (at least in their actual formulation). Nevertheless, it is also demonstrated that the incorporation of the chitosan layer, not only enhances the mechanical properties of the dry multilayer films but also the mucoadhesion is not compromised despite the formation of the PECs.

According to the drug release profiles (Fig. 9), when the drug is physically mixed with the polymers, the release of the TFV occurs faster in the films prepared with xanthan gum than in the films prepared with karaya gum. According to the resistivity values presented in Fig. 6, EKC is in general more resistive than EXC thus the SVF moves faster in the EXC films. However, the loss angle profile (Fig. 5f) indicates that the dipoles become stacked and entrapped within the viscous polymeric chain. These two effects balance the kinetics of the drug release profiles in the absence of the inorganic drug release regulator.

When the drug is loaded inside the inorganic release regulator, the opposite behavior was found, with a faster release in the films produced with karaya gum. From the electrochemical characterization, it was demonstrated that in EKC films the presence of the inorganic drug release regulator enhanced the ionic mobility of the SVF, which explains the faster release of the drug in this case and is also related to the formation of PECs. As Cazorla-Luna, Martin-Illana, Notario-Perez, Miguel Bedoya, et al. (2020) demonstrated, the better is the crosslinking between the polyanions, the slower is the release. According to the Weibull's model, in this case the diffusion of the TFV follows similar paths throughout the polymeric matrix independently of the biopolymer used (similar b values). However, as mentioned above, the presence of the inorganic drug regulator favors the formation of the PECs in the EKC films thus minimizing the resistivity values with time which in this case is translated into faster drug diffusion despite the highest resistivity of the EKC films (the lower $\underline{a}$ values indicates faster kinetics). The obtained results therefore suggest that the PECs formed in the EKC films should be less crosslinked than in the EXC films thus allowing the faster diffusion of the drug when it is loaded inside the particles. This is also evidenced by the low variation in the mobile charges observed with time of the EXC films indicating that films based in this biopolymer are promising candidates for multicomponent films because the incorporation of different drug release regulators does not alter significantly the hydration dynamics and acts in beneficial of a slow release.

5. Conclusions

Trilayer films containing karaya gum, pectin and xanthan gum as low-swellable and structural polymers, a chitosan mucoadhesion enhancer and two drug release regulators (organic and inorganic in nature) have been successfully produced and characterized with a focus on their application as mucoadhesive films for vaginal drug delivery. The incorporation of the chitosan-based film to enhance the mucoadhesion in the trilayer films lead to lower SR than the bilayer films in the case of the use of karaya and xanthan gums and slightly higher when pectin is used. This event can be related with the formation of PECs between the biopolymer and chitosan leading to a decrease of the high swelling of the natural polymers xanthan and karaya gums and to the control of the pectin destructuring when in contact with the SVF.

The application of electrochemical techniques to discern the hydration dynamics, both in the SVF penetration and in the drug release kinetics has been proved successful. By means of EIS, the ionic mobility of the films was identified and related with the formation of the PECs. The addition of an inorganic drug release regulator enhances the water penetration of the films manufactured with karaya gum and favors the formation of the PECs. However, the PECs do not allow retaining the drug molecules, a fact that is attributed to the low molecular weight of these complexes because of the weakening effect of the particles on the polymeric chains. As a conclusion, trilayer films based on karaya gum have shown the most promising characteristics for being translated to an ex-vivo and in-vivo applications although their mechanical properties should be moderately improved in future pharmaceutical formulations.

CRediT authorship contribution statement

Araceli Martín-Illana: Investigation, Resources. **Eva Chinarro:** Methodology, Formal analysis. **Raul Cazorla-Luna:** Investigation, Software. **Fernando Notario-Perez:** Investigation, Visualization. **M.D. Veiga-Ochoa:** Funding acquisition, Project administration. **Juan**

Rubio: Validation, Visualization, Supervision. **Aitana Tamayo:** Conceptualization, Data curation, Formal analysis, Investigation, Writing – original draft, Writing – review & editing.

Declaration of competing interest

None.

Acknowledgements

This work was supported by the Spanish Research Agency and the European Regional Development Fund (AEI/FEDER, UE), grant number MAT2016-76416-R. We are grateful to the Carnes Barbero slaughterhouse (El Barraco, Ávila, Spain) for supplying the biological samples. We would also like to thank María Hernando, veterinarian at the Junta de Castilla y León, for verifying the suitability of the biological samples.

Appendix A. Supplementary data

Supplementary data to this article can be found online at https://doi.org/10.1016/j.carbpol.2021.118958.

References

Baah-Dwomoh, A., McGuire, J., Tan, T., & De Vita, R. (2016). Mechanical properties of female reproductive organs and supporting connective tissues: A review of the current state of knowledge. *Applied Mechanics Reviews, 68*(6).

Bassi da Silva, J., Ferreira, S. B. D. S., Reis, A. V., Cook, M. T., & Bruschi, M. L. (2018). Assessing mucoadhesion in polymer gels: The effect of method type and instrument variables. *Polymers, 10*(3), 254.

Bigucci, F., Luppi, B., Cerchiara, T., Sorrenti, M., Bettinetti, G., Rodriguez, L., & Zecchi, V. (2008). Chitosan/pectin polyelectrolyte complexes: Selection of suitable preparative conditions for colon-specific delivery of vancomycin. *European Journal of Pharmaceutical Sciences, 35*(5), 435–441.

Bueno, V. B., Bentini, R., Catalani, L. H., & Petri, D. F. S. (2013). Synthesis and swelling behavior of xanthan-based hydrogels. *Carbohydrate Polymers, 92*(2), 1091–1099.

Cao, T. L., & Song, K. B. (2019). Active gum karaya/Cloisite Na+ nanocomposite films containing cinnamaldehyde. *Food Hydrocolloids, 89*, 453–460.

Capaccioli, S., Lucchesi, M., Casalini, R., Rolla, P., & Bona, N. (2000). Influence of the wettability on the electrical response of microporous systems. *Journal of Physics D: Applied Physics, 33*(9), 1036.

Cazorla-Luna, R., Notario-Perez, F., Martin-Illana, A., Ruiz-Caro, R., Tamayo, A., Rubio, J., & Veiga, M. D. (2019). Chitosan-based mucoadhesive vaginal tablets for controlled release of the anti-HIV drug tenofovir. *Pharmaceutics, 11*(1), 20.

Cazorla-Luna, R., Martin-Illana, A., Notario-Perez, F., Bedoya, L. M., Tamayo, A., Ruiz-Caro, R., & MD, V. (2020). Vaginal polyelectrolyte layer-by-layer films based on chitosan derivatives and Eudragit® S100 for pH responsive release of tenofovir. *Marine Drugs, 18*(44).

Cazorla-Luna, R., Martin-Illana, A., Notario-Perez, F., Miguel Bedoya, L., Tamayo, A., Ruiz-Caro, R., & Veiga, M.-D. (2020). Vaginal polyelectrolyte layer-by-layer films based on chitosan derivatives and eudragit S100 for pH responsive release of tenofovir. *Marine Drugs, 18*(1).

Cazorla-Luna, R., Notario-Pérez, F., Martín-Illana, A., Bedoya, L.-M., Tamayo, A., Rubio, J., & Veiga, M.-D. (2020). Development and in vitro/ex vivo characterization of vaginal mucoadhesive bilayer films based on ethylcellulose and biopolymers for vaginal sustained release of tenofovir. *Biomacromolecules, 21*(6), 2309–2319.

Cazorla-Luna, R., Martin-Illana, A., Notario-Pérez, F., Ruiz-Caro, R., & Veiga, M.-D. (2021). Naturally occurring polyelectrolytes and their use for the development of complex-based mucoadhesive drug delivery systems: An overview. *Polymers, 13*(14), 2241.

Christensen, B. J., Coverdale, T., Olson, R. A., Ford, S. J., Garboczi, E. J., Jennings, H. M., & Mason, T. O. (1994). Impedance spectroscopy of hydrating cement-based materials: Measurement, interpretation, and application. *Journal of the American Ceramic Society, 77*(11), 2789–2804.

Ćirić, A., Medarević, Đ., Čalija, B., Dobričić, V., Mitrić, M., & Djekic, L. (2020). Study of chitosan/xanthan gum polyelectrolyte complexes formation, solid state and influence on ibuprofen release kinetics. *International Journal of Biological Macromolecules, 148*, 942–955.

Cost, M., Dezzutti, C. S., Clark, M. R., Friend, D. R., Akil, A., & Rohan, L. C. (2012). Characterization of UC781-tenofovir combination gel products for HIV-1 infection prevention in an ex vivo ectocervical model. *Antimicrobial Agents and Chemotherapy, 56*(6), 3058–3066.

Czechowska-Biskup, R., Jarosińska, D., Rokita, B., Ulański, P., & Rosiak, J. M. (2012). Determination of degree of deacetylation of chitosan-comparision of methods. *Progress on Chemistry and Application of Chitin and its Derivatives, 17*, 5–20.

Dash, S., Murthy, P. N., Nath, L., & Chowdhury, P. (2010). Kinetic modeling on drug release from controlled drug delivery systems. *Acta Poloniae Pharmaceutica, 67*(3), 217–223.

Dotelli, G., & Mari, C. (2001). The evolution of cement paste hydration process by impedance spectroscopy. *Materials Science and Engineering: A, 303*(1–2), 54–59.

Fan, M. D., Kramzer, L. F., Hillier, S. L., Chang, J. C., Meyn, L. A., & Rohan, L. C. (2017). Preferred physical characteristics of vaginal film microbicides for HIV prevention in Pittsburgh women. *Archives of Sexual Behavior, 46*(4), 1111–1119.

Ilhan-Ayisigi, E., & Yesil-Celiktas, O. (2018). Silica-based organic-inorganic hybrid nanoparticles and nanoconjugates for improved anticancer drug delivery. *Engineering in Life Sciences, 18*(12), 882–892.

Ishihara, M., Kishimoto, S., Nakamura, S., Sato, Y., & Hattori, H. (2019). Polyelectrolyte complexes of natural polymers and their biomedical applications. *Polymers, 11*(4), 672.

Karim, Q. A., Karim, S. S. A., Frohlich, J. A., Grobler, A. C., Baxter, C., Mansoor, L. E., & Omar, Z. (2010). Effectiveness and safety of tenofovir gel, an antiretroviral microbicide, for the prevention of HIV infection in women. *Science, 329*(5996), 1168–1174.

Kaur, G., Grewal, J., Jyoti, K., Jain, U. K., Chandra, R., & Madan, J. (2018). Oral controlled and sustained drug delivery systems: concepts, advances, preclinical, and clinical status. In *Drug targeting and stimuli sensitive drug delivery systems* (pp. 567–626). Elsevier.

Kocherbitov, V., Ulvenlund, S., Briggner, L.-E., Kober, M., & Arnebrant, T. (2010). Hydration of a natural polyelectrolyte xanthan gum: Comparison with non-ionic carbohydrates. *Carbohydrate Polymers, 82*(2), 284–290.

Kosmidis, K., Argyrakis, P., & Macheras, P. (2003). A reappraisal of drug release laws using Monte Carlo simulations: The prevalence of the weibull function. *Pharmaceutical Research, 20*(7), 988–995.

Kumar, L., Reddy, M., Shirodkar, R., Pai, G., Krishna, V., & Verma, R. (2013). Preparation and characterisation of fluconazole vaginal films for the treatment of vaginal candidiasis. *Indian Journal of Pharmaceutical Sciences, 75*(5), 585.

Lankalapalli, S., & Kolapalli, V. (2009). Polyelectrolyte complexes: A review of their applicability in drug delivery technology. *Indian Journal of Pharmaceutical Sciences, 71*(5), 481.

Lei, L., Liu, X., Shen, Y.-Y., Liu, J.-Y., Tang, M.-F., Wang, Z.-M., & Cheng, L. (2011). Zero-order release of 5-fluorouracil from PCL-based films featuring trilayered structures for stent application. *European Journal of Pharmaceutics and Biopharmaceutics, 78*(1), 49–57.

Maciel, V. B. V., Yoshida, C. M., & Franco, T. T. (2015). Chitosan/pectin polyelectrolyte complex as a pH indicator. *Carbohydrate Polymers, 132*, 537–545.

Martín-Illana, A., Notario-Pérez, F., Cazorla-Luna, R., Ruiz-Caro, R., & Veiga, M. D. (2019). Smart freeze-dried bigels for the prevention of the sexual transmission of HIV by accelerating the vaginal release of tenofovir during intercourse. *Pharmaceutics, 11*(5), 232.

Martin-Illana, A., Cazorla-Luna, R., Notario-Pérez, F., Ruiz-Caro, R., Bedoya, L. M., Veiga-Ochoa, M. D., & Tamayo, A. (2020). Amino functionalized micro-mesoporous hybrid particles for the sustained release of the antiretroviral drug tenofovir. *Materials, 13*(16), 3494.

Martín-Illana, A., Cazorla-Luna, R., Notario-Pérez, F., Bedoya, L. M., Rubio, J., Tamayo, A., & Veiga, M. D. (2021). Smart vaginal bilayer films of tenofovir based on Eudragit® L100/natural polymer for the prevention of the sexual transmission of HIV. *International Journal of Pharmaceutics, 602*, Article 120665.

McCoy, C. F., Millar, B. G., Murphy, D. J., Blanda, W., Hansraj, B., Devlin, B., & Boyd, P. (2019). Mechanical testing methods for drug-releasing vaginal rings. *International Journal of Pharmaceutics, 559*, 182–191.

Meka, V. S., Sing, M. K., Pichika, M. R., Nali, S. R., Kolapalli, V. R., & Kesharwani, P. (2017). A comprehensive review on polyelectrolyte complexes. *Drug Discovery Today, 22*(11), 1697–1706.

Melegari, C., Bertoni, S., Genovesi, A., Hughes, K., Rajabi-Siahboomi, A. R., Passerini, N., & Albertini, B. (2016). Ethylcellulose film coating of guaifenesin-loaded pellets: A comprehensive evaluation of the manufacturing process to prevent drug migration. *European Journal of Pharmaceutics and Biopharmaceutics, 100*, 15–26.

Mesquita, L., Galante, J., Nunes, R., Sarmento, B., & das Neves, J. (2019). Pharmaceutical vehicles for vaginal and rectal administration of anti-HIV microbicide nanosystems. *Pharmaceutics, 11*(3), 145.

Munarin, F., Tanzi, M. C., & Petrini, P. (2012). Advances in biomedical applications of pectin gels. *International Journal of Biological Macromolecules, 51*(4), 681–689.

Munday, D. L., & Cox, P. J. (2000). Compressed xanthan and karaya gum matrices: Hydration, erosion and drug release mechanisms. *International Journal of Pharmaceutics, 203*(1–2), 179–192.

Murata, Y., Maida, C., & Kofuji, K. (2019). Drug release profiles and disintegration properties of pectin films. *Materials, 12*(3), 355.

Notario-Pérez, F., Martín-Illana, A., Cazorla-Luna, R., Ruiz-Caro, R., Bedoya, L.-M., Tamayo, A., & Veiga, M.-D. (2017). Influence of chitosan swelling behaviour on controlled release of tenofovir from mucoadhesive vaginal systems for prevention of sexual transmission of HIV. *Marine Drugs, 15*(2), 50.

Notario-Pérez, F., Cazorla-Luna, R., Martín-Illana, A., Galante, J., Ruiz-Caro, R., das Neves, J., & Veiga, M.-D. (2020). Design, fabrication and characterisation of drug-loaded vaginal films: State-of-the-art. *Journal of Controlled Release, 327*(10), 477–499.

Owen, D. H., & Katz, D. F. (1999). A vaginal fluid simulant. *Contraception, 59*(2), 91–95.

Padil, V. V., Wacławek, S., Černík, M., & Varma, R. S. (2018). Tree gum-based renewable materials: Sustainable applications in nanotechnology, biomedical and environmental fields. *Biotechnology Advances, 36*(7), 1984–2016.

Papadopoulou, V., Kosmidis, K., Vlachou, M., & Macheras, P. (2006). On the use of the weibull function for the discernment of drug release mechanisms. *International Journal of Pharmaceutics, 309*(1–2), 44–50.

Ramakrishnan, R., Pa-dil, V., Wacławek, S., Černík, M., & Varma, R. (2021). Eco-friendly and economic, adsorptive removal of cationic and anionic dyes by bio-based karaya

gum—chitosan sponge. *Polymers, 2021*(13), 251. s Note: MDPI stays neu-tral with regard to jurisdictional claims in ….

Ranganathan, P., Mutharani, B., Chen, S.-M., & Sireesha, P. (2019). Biocompatible chitosan-pectin polyelectrolyte complex for simultaneous electrochemical determination of metronidazole and metribuzin. *Carbohydrate Polymers, 214*, 317–327.

Saunders, B. R., & Vincent, B. (1999). Microgel particles as model colloids: Theory, properties and applications. *Advances in Colloid and Interface Science, 80*(1), 1–25.

Sriamornsak, P., Thirawong, N., Weerapol, Y., Nunthanid, J., & Sungthongjeen, S. (2007). Swelling and erosion of pectin matrix tablets and their impact on drug release behavior. *European Journal of Pharmaceutics and Biopharmaceutics, 67*(1), 211–219.

Tamayo, A., Mazo, M. A., Veiga, M. D., Ruiz-Caro, R., Notario-Pérez, F., & Rubio, J. (2017). Drug kinetics release from eudragit – Tenofovir@SiOC tablets. *Materials Science and Engineering: C, 75*, 1097–1105.

UNAIDS_Secretary_General. (2021). *Addressing inequalities and getting back on track to end AIDS by 2030*. United Nations.

Vallet-Regí, M., Colilla, M., & González, B. (2011). Medical applications of organic–inorganic hybrid materials within the field of silica-based bioceramics. *Chemical Society Reviews, 40*(2), 596–607.

Vinchhi, P., Rawal, S. U., & Patel, M. M. (2021). Biodegradable hydrogels. In *Drug Delivery Devices and Therapeutic Systems* (pp. 395–419). Elsevier.

Wang, P., Li, Y., Zhang, C., Que, F., Weiss, J., & Zhang, H. (2020). Characterization and antioxidant activity of trilayer gelatin/dextran-propyl gallate/gelatin films: Electrospinning versus solvent casting. *Lwt, 128*, Article 109536.

Wu, Q., & Li, L. (2020). Thermal sensitive Poloxamer/Chitosan hydrogel for drug delivery in vagina. *Materials Research Express, 7*(10), Article 105401.

Yadav, V. K., Gupta, A., Kumar, R., Yadav, J. S., & Kumar, B. (2010). Mucoadhesive polymers: Means of improving the mucoadhesive properties of drug delivery system. *Journal of Chemical and Pharmaceutical Research, 2*(5), 418–432.

Yu, X., Yi, B., Liu, F., & Wang, X. (2008). Prediction of the dielectric dissipation factor tan δ of polymers with an ANN model based on the DFT calculation. *Reactive and Functional Polymers, 68*(11), 1557–1562.